SANDIA REPORT
SAND2012-7383
Unlimited Release
Printed August 2012

Statistics of particle time-temperature histories: Progress report for August 2012

John C. Hewson, David O. Lignell, Guangyuan Sun

Prepared by
Sandia National Laboratories
Albuquerque, New Mexico 87185 and Livermore, California 94550

Sandia National Laboratories is a multi-program laboratory managed and operated by Sandia Corporation, a wholly owned subsidiary of Lockheed Martin Corporation, for the U.S. Department of Energy's National Nuclear Security Administration under contract DE-AC04-94AL85000.

Issued by Sandia National Laboratories, operated for the United States Department of Energy by Sandia Corporation.

Available to DOE and DOE contractors from
U.S. Department of Energy
Office of Scientific and Technical Information
P.O. Box 62
Oak Ridge, TN 37831

Telephone: (865) 576-8401
Facsimile: (865) 576-5728
E-Mail: reports@adonis.osti.gov
Online ordering: http://www.osti.gov/bridge

Available to the public from
U.S. Department of Commerce
National Technical Information Service
5285 Port Royal Rd.
Springfield, VA 22161

Telephone: (800) 553-6847
Facsimile: (703) 605-6900
E-Mail: orders@ntis.fedworld.gov
Online order: http://www.ntis.gov/help/ordermethods.asp?loc=7-4-0#online

SAND2012-7383
Unlimited Release
Printed August 2012

Statistics of particle time-temperature histories: Progress report for August 2012

John C. Hewson
Sandia National Laboratories
P.O. Box 5800
Albuquerque, New Mexico 87185

David O. Lignell, Guangyuan Sun
Brigham Young University
Provo, Utah 84602

Abstract

Progress toward predictions of the statistics of particle time-temperature histories is presented. The joint statistics of a scalar like the temperature and an exposure time scale are of interest. We have related these quantities to statistics of conserved scalars, their gradients and their diffusive time scales. Future work will apply the one-dimensional turbulence (ODT) model to evaluate the suitability of these statistics to predicting particle time-temperature histories. To that end, we have reported on past performance of the ODT model and have implemented a Lagrangian particle tracking capability into the ODT code. The results of ODT-driven particle dispersion have been compared with classical experimental data, and preliminary statistics of particle evolution in reacting flows are also reported.

Acknowledgements

This work is supported by the Defense Threat Reduction Agency (DTRA) under their Counter-Weapons of Mass Destruction Basic Research Program in the area of Chemical and Biological Agent Defeat under award number HDTRA1-11-4503I to Sandia National Laboratories. The authors would like to express their appreciation for the guidance provided by Dr. Suhithi Peiris to this project and to the Science to Defeat Weapons of Mass Destruction program.

Introduction

One approach to neutralize biological agents involves the use of devices that provide either a thermal or chemical environment that is lethal to the biological agent. Such an environment is typically provided through an explosive dispersal process that is expected to cover much of the area of interest, but this blast can also displace agents in a manner that can reduce their exposure to the lethal environment. This project addresses the post-blast-phase mixing between the biological agents, the environment that is intended to neutralize them, and the ambient environment that dilutes it. In particular, this work addresses the mixing between the aerosols and high-temperature (or otherwise toxic) gases, and seeks to understand mixing environments that insure agent kill. Currently, turbulent mixing predictions by computational fluid dynamics (CFD) provide a certain degree of predictivity, and other programs are addressing research in this area. A significant challenge in standard CFD modeling is the accurate prediction of fine-scale fluid-aerosol interactions. Here we study the statistics of particle interactions with high-temperature gases by employing a stochastic modeling approach that fully resolves the range of states (by resolving the full range of turbulent scales down to the molecular mixing scales). This stochastic approach is referred to as the one-dimensional turbulence (ODT) model and will provide a new understanding of low-probability events including the release of a small fraction of biological agents. These crucial low-probability events constitute the tails of a probability distribution function of agent release which are particularly difficult to model using existing approaches.

Of relevance to neutralizing biological agents is the fact that some time-integrated exposure is generally required. This work seeks to develop an understanding of time-integrated particle-environment interactions by quantifying the relationship between these histories and predictable quantities. Here predictable quantities are those that can be predicted in the context of a CFD simulation that does not resolve fully the range of length and time scales and thus requires some modeling of the particle time-temperature histories. As will be discussed in the Statistics section below, this involves characterizing the relative motions of the particles and the high-temperature gases and relating these characteristics to predictable quantities. This will provide guidance on the modeling requirements for physics-based prediction of the particle time-temperature histories.

The primary method by which we will obtain statistics regarding the relative motions of the particles and the high-temperature gases is the ODT model [1-3]. In the ODT model, the full range of length scales is resolved on a one-dimensional domain that is evolved at the finest time scales. This allows a direct simulation of all diffusive and chemical processes along a notional line-of-sight through the turbulent flow. Turbulent advection is incorporated through stochastic eddy events imposed on the domain. The turbulent energy cascade arises in the Navier-Stokes equations through the nonlinear interaction of three-dimensional vorticity. This cascade results in length scale reduction and increased gradients. The ODT model incorporates these effects through “triplet maps,” the size, rate, and location of which are determined by the state of a locally evolved instantaneous velocity field that provides a local measure of the rate of the turbulent cascade. The evolution of eddy events implemented through triplet maps reproduces key aspects of the turbulent cascade. That is, large scale fluctuations cascade to smaller scale fluctuations with increasing rate, while the magnitude of the fluctuations decreases appropriately, reproducing typical spectral scaling laws. In this work we briefly review past applications of the ODT model that provide confidence that we can predict quantities of interest in the flow evolution in the

section on ODT model comparisons with canonical flows. Then we describe the recent implementation of Lagrangian particles into the ODT model. Finally, we provide a look forward with some statistics of interest from preliminary simulations with Lagrangian particles and describe the next steps in the understanding of particle time-temperature histories.

Before proceeding further, it is important to put the present ODT-based approach into the context of more traditional CFD simulation techniques. For filtered solutions of the Navier-Stokes equations (traditional large-eddy simulation or LES, Reynolds-averaged Navier-Stokes or RANS), only lower moments (like averages) of quantities of interest are available while there is no information about the tails of the distribution like the pockets of gas with the lowest temperatures. The present ODT modeling approach provides the information necessary to construct the required full distribution of states by explicitly resolving the fine-scale processes. At the same time, traditional CFD is better able to handle complicated geometric environments, in part because these methods are developed for those environments and in part because the simplifications employed in the ODT model are aimed directly at avoiding geometric complexity. In this sense, ODT is completely complementary to approaches like RANS and LES. RANS and LES have the greatest fidelity toward the large-scale dynamics while all of the small-scale processes are subsumed within models. Conversely, ODT prescribes a model for the large-scale dynamics, but completely resolves the small-scale processes including the statistically rare events. The link between these two complementary approaches is as follows. The driving force in ODT for the modeled large-scale mixing is the overall shear energy of the flow. This shear energy, in the form of an overall velocity gradient, gives a time scale for the turbulent cascade of large-scale fluctuations to the diffusive scales. Also input to an ODT simulation is a length scale and some information about boundary conditions. These quantities required for an ODT simulation are those that tend to be well predicted by traditional CFD. Since the output from an ODT simulation includes information not accessible from traditional CFD, these approaches are nicely complementary.

Summary of Progress to July 1012

In the project year from April 2011 to April 2012 three specific tasks were identified (note that the order is reversed relative to the original statement of work just because the documentation flows more naturally in this report):

Task 1: Define statistical data requirements.

Task 2: Compare ODT predictions for jet mixing.

Task 3: Add particle tracking capability to ODT code.

Each of these tasks has been completed, although as work progresses continued development is expected in each of these core areas. For example, as statistics of particle time-temperature histories are analyzed we expect results to point to new statistical quantities of interest. Also, while we have implemented the particle tracking capabilities within the ODT code, we are continuing evaluation of the implemented models and considering the consequences of alternate implementations (in particular the validation of the particle heat transfer model discussed in the Particle model implementation section is not yet completed and might suggest alternate model forms). Details regarding the work accomplished in completing each of these tasks will be described in the following three sections.

In the project year from April 2012 to April 2013 three additional tasks are targeted:

Task 4: Carry out free-shear flow simulations.

Task 5: First-stage analysis of free-shear flows: correlation coefficients.

Task 6: Compare ODT predictions for particle-wall deposition.

Preliminary results from Task 4 will be reported in the final sections. In addition to the proposed tasks, we expect to perform some additional validation of the particle model implementation within the ODT code in the area of dispersion in shear flows in conjunction with Task 4.

Statistics of particle time-temperature histories

It is known that biological agents can be neutralized through exposure to sufficiently high temperatures or chemically-hostile environments for a sufficient duration. In the first stages of this work we will focus on thermal inactivation as a model with the premise that net particle heating to some critical temperature, T_{cr}, is required to neutralize the particle. With this premise, to heat a particle to T_{cr} one should consider a simplified particle temperature equation

$$\frac{dT_p}{dt} = \frac{\left(T_g - T_p\right)}{\tau_h} \quad , \tag{1}$$

where T_g and T_p are the gas and particle temperatures, respectively, and τ_h is the characteristic heating time for the particle. This heating time scale, τ_h, will depend on the particle size, its fractal nature, its thermal characteristics, the gas thermal characteristics and its slip velocity relative to the gas among other things. In the present work, we take to τ_h be given except for the consideration of its slip velocity and, in particular, correlations between its slip velocity and the gas temperature field. A similar expression for exposure to a gas-phase chemical species, C_g, that has deleterious effects on the particle might be written

$$\frac{dC_p}{dt} = \frac{C_g}{\tau_c} \quad , \tag{2}$$

where τ_c is the characteristic time for diffusion of C_g to the particle and C_p counts the accumulation to a lethal dosage. Since Eq. (2) is so similar to (1) the bulk of the discussion will refer to temperature evolution with the understanding that the discussion applies to both.

With Eq. (1) forming the basic particle evolution model at this stage with $T_p > T_{cr}$ indicating a neutralized particle, an objective would be to determine the probability that the particle temperature exceeds the critical temperature, Prob($T_p > T_{cr}$). With this objective, in addition to the heating time scale, the important quantity that determines the particle temperature evolution is the gas temperature that a particle 'sees,' the environment temperature. There are two components to this observed gas temperature: the statistics of the observed gas temperature and the characteristic time scales of temperature extrema. To illustrate this, we discuss an environment temperature, T_g, that varies as a square wave between two values, one temperature below T_{cr} and one temperature above T_{cr}. During each segment of the square wave, the particle temperature exponentially approaches the environment temperature with a time constant τ_h

$$\frac{\left(T_{p,f}-T_g\right)}{\left(T_{p,0}-T_g\right)}=e\left(-\frac{\Delta t}{\tau_h}\right). \tag{3}$$

Here, $T_{p,f}$ and $T_{p,0}$ are the initial and final particle temperatures, respectively for each wave segment of duration Δt. If τ_h is sufficiently small *and* if T_g is sufficiently large, then a single square wave might neutralize the particle. This is demonstrated in the upper panel of Figure 1. If this does not occur in a single square wave, then a sequence of multiple square waves might neutralize the particle *if* the duration between high temperature environments is smaller than the duration between low temperature environments as indicated in the middle and lower panes of Figure 1. Thus, to predict Prob($T_p > T_{cr}$) involves predicting the joint statistics of temperature and time scales. Of course, within a turbulent flow field the temperatures and time scales do not have a simple bimodal-delta-function distribution. These statistics are expressed in terms of the joint probability density function $P(T_g, \Delta t)$. This will be discussed in the following subsections after a comment regarding more complex particle neutralization criteria.

It is straightforward to employ nonlinear particle response models, and those nonlinearities will alter the statistical requirements associated with neutralization. For example, if variations in water vapor pressure are critical, these introduce a nonlinearity (vapor pressure being roughly Arrhenius in temperature) that could be tracked within the particle context. In this case, the particle neutralization criteria might instead be written Prob($P_{H2O}(T_p) > P_{cr}$) where $P_{H2O}(T_p)$ indicates the nonlinear relationship between the vapor pressure and particle temperature.

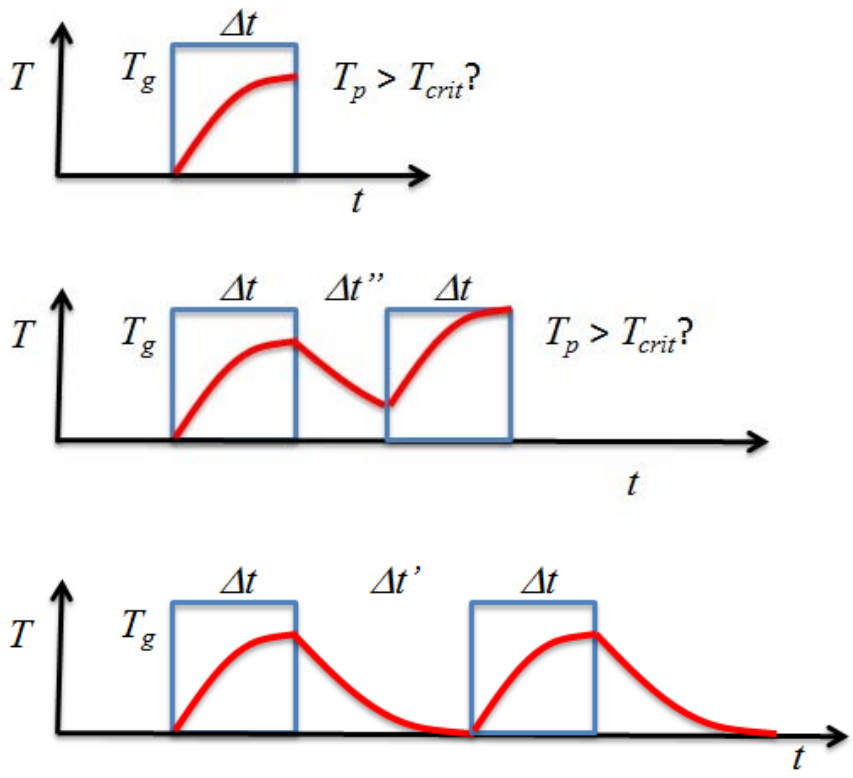

Figure 1. Particle temperature response to hypothetical gas-phase temperature following a square wave pattern with high temperature durations Δt and low temperature durations $\Delta t'$. Depending on T_g and Δt relative to T_{crit} and τ_p, the particle temperature may or may not exceed T_{crit}.

Statistics of gas temperatures

To leading order the temperature distribution is important. Generally in CFD the full distribution cannot be predicted without fully resolving the flow, so the distribution will need to be related to moments of the distribution: the mean temperature, its variance and the higher moments. The higher moments become more significant in identifying probabilities near the extremes of the temperature distribution. That is, near the edges of the turbulent flame when the typical temperature is not sufficiently high, we rely on intermittent excursions of high temperatures to neutralize particles. The probability of these intermittent high temperatures is described by the tails of the temperature PDF. Also important are the low temperature tails of the temperature distribution that might be associated with improbable failures to neutralize particles. In situations where mixing of hot and cool gases occurs in conjunction with heat losses, to walls for example, if the gas cooling occurs before mixing with cool gases containing particles, there might be a failure to neutralize particles. Higher moments like the skewness and kurtosis will also alter the relative durations of specific temperatures. This would alter the Δt associated with high and low temperature regions as in the square wave example.

Significant parameters determining temperature statistics include:

- Domain average temperature prior to heat losses, $T_{av,0}$, relative to T_{cr}.
- Magnitude of initial temperature fluctuations relative to $T_{av,0}$ - T_{cr}.
- Characteristic (wall) heat loss temperature, T_w, relative to T_{cr}.
- Time scale for mixing of hot gases with particle-containing gases relative to time scale for particle heating.
- Time scale for mixing of hot gases with particle-containing gases relative to time scale for heat losses.
- Time scale for mixing of hot gases with particle-containing gases relative to time scale for long-time heat release (fuel-oxidizer mixing or energetic particle burning).

It is important to note here that during the flow evolution, temperature inhomogeneities associated with unmixedness are dissipated, so that the time scale for mixing of hot gases with particle-containing gases is effectively a time scale for temperature homogenization. At the same time, the time scale for heat losses introduces inhomogeneities in the temperature field by introducing cool fluid elements. Depending on how distributed long-time heat release is this could introduce additional temperature inhomogeneities.

Figure 2 shows an example of a temperature PDF computed using ODT for a buoyant vertical wall fire. Ethylene fuel is fed through the wall at a rate of 390 L/min at 300 K. The PDF is shown at several distances from the wall at a height of 1.8 m. As the wall is approached the PDF peaks at higher temperatures. Away from the wall, the PDF peaks at lower temperatures due to air entrainment. The 0.15 m curve shows a bimodal distribution with an initial spike at the air temperature. This would also occur very close to the wall (not shown) where peaks would occur at the cold fuel temperature and the hot flame temperature.

Time scales for temperature fluctuations

In addition to the distribution of T_g, it is necessary to predict the time scales for temperature fluctuations. To understand this, it is instructive to describe the evolution of T_g from a Lagrangian reference frame moving with the particle written as

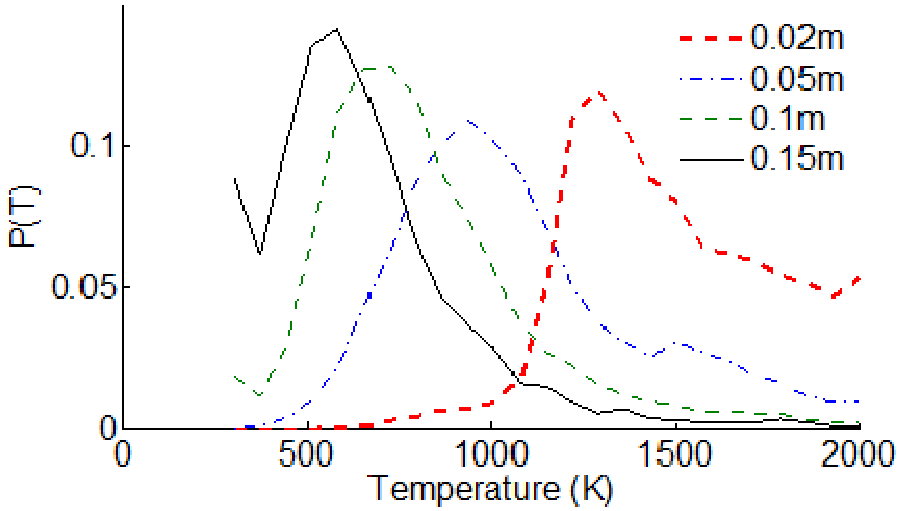

Figure 2. PDF of temperature at distances from a vertical wall fire at a height of 1.8 m computed using the present ODT code.

$$\left.\frac{dT_g}{dt}\right|_p = \left(v_p - v_g\right)\cdot\nabla T_g + \frac{DT_g}{Dt}. \tag{4}$$

The first term on the right-hand side of Eq. (4) describes the change in the observed temperature as the particle moves relative to the gas-phase field. This is particularly relevant for large ballistic particles (large Stokes numbers) that can move rapidly through the gas-phase field. This term involves the temperature gradient that will need to be understood at dissipative scales. The second term is written in terms of the substantial derivative for a fluid element

$$\frac{DT_g}{Dt} = \frac{dT_g}{dt} + v_g\cdot\nabla T_g \tag{5}$$

that describes the change in the gas temperature of that fluid element. This term is particularly relevant for small particles (small Stokes numbers) that follow the gas-phase flow since the velocity difference, $v_p - v_g$, approaches zero for these particles. It is noted here that the temperature conservation equation can be used to replace the right-hand side of Eq. (5) with

$$\frac{DT_g}{Dt} = \nabla\cdot\left(D_T\nabla T_g\right) + \dot{q} \tag{6}$$

that shows the second term of Eq. (4) also depends on processes, diffusion and reaction, that occur at diffusive scales ($\dot{q}$ is the heat release rate).

To understand the statistics of the temperature and its time scale that the particles see, it is necessary to understand the quantities appearing in the right-hand sides of Eq. (4) and these are the subject of the following paragraphs. It should be noted that for strongly accelerating flows with large temperature gradients, the first term in Eq. (4) might be the dominant term even for particles with small Stokes numbers.

It has been noted that both sets of terms in Eq. (4) involve statistics of temperature gradients, diffusive processes or source terms. In general it is difficult to determine reactive scalar gradients within the context of CFD, and in the present work we will focus on relating these to the statistics of conserved scalars, their gradients and dissipation. That is, when the temperature is a reacting scalar, it will be related to other conserved scalars. A standard method of doing this is to relate the reactive scalars to the so-called mixture fraction variable that describes the (elemental) fraction of the fluid that originated in the one stream. Conditional-moment closure [4] and flamelet methods [5] are based on these relationships.

When we are interested in the temperature gradient as in the first term in Eq. (4), the conserved scalar dissipation rate

$$\chi = 2D\left|\nabla \xi\right|^2 \tag{7}$$

is the appropriate quantity for which to collect statistics. In Eq. (7) D is the diffusion coefficient appropriate for the scalar and ξ is the conserved scalar. The scalar dissipation rate is known to be closely related to the rate of turbulence production and is commonly modeled in CFD and LES contexts. The square root of the scalar dissipation rate gives the scalar gradient. It should be noted that the units of the scalar gradient can be thought of as "crossings per path length," and in the context of ballistics particles moving relative to the fluid, the frequency of crossings corresponding to specific temperature values are the objective. To refine this one step further, if we conditionally average the scalar gradient (dissipation rate) on the mixture fraction value of interest (there being a one-to-one mapping to the temperature of interest) we can obtain the frequency (in crossings per path length) for a given temperature iso-surface. Thus, the time scale associated with a scalar sampled at η (conditionally averaged at η) is

$$\Delta t = \left[\left(v_p - v_g\right)\left\langle \nabla \xi \,|\, \eta \right\rangle\right]^{-1} \tag{8}$$

where the conditioning value will be associated with different gas temperatures. We can make this more clear by writing

$$\Delta t\left(T_g\right) = \left[\left(v_p - v_g\right)\left\langle \nabla \xi \,|\, \eta\left(T_g\right)\right\rangle\right]^{-1} \tag{9}$$

where the functional dependence of Δt and η on T_g is made explicit.

As discussed above, for the first term in Eq. (4) we are looking for the joint probability density function $P(T_g, \Delta t)$. With the results of the preceding paragraph we can rewrite our objective as the probability of a scalar and its gradient conditioned on specific values of T_g

$$P\left(\xi, \nabla \xi \,|\, \eta\left(T_g\right)\right) \tag{10}$$

It is worth noting that $\langle \nabla \xi \,|\, \eta \rangle$ can also be interpreted as "isoscalar surface area per volume" and this is the basis of another class of models referred to as flame-surface density models [6, 7].

Another point that is worth noting is that conditional averages of the scalar dissipation rate are known to approach zero at extrema. If the temperature is a non-reacting scalar, this informs us that the magnitude of its gradient and the number of crossings in a trajectory approach zero at the scalar maxima and minima. Thus, the conditional average of the scalar gradient has the expected behavior as the maximum temperature is approached.

When particles are small, the second term in Eq. (4) is important. This term is characterized by the temperature reactive and diffusive processes in the gas phase as indicated in Eq. (6) and represents the change of temperature following a fluid element. In prior work, this evolution of a reactive scalar relative to fluid elements (that aerosol particles follow) was identified with the diffusive motion of flames through studies with both ODT and DNS [8, 9]. Figure 3 shows soot contours with the flame surface contour line colored by the relative velocity between the flame and the soot. In red regions, the soot is transported towards the flame, and in blue regions the soot is transported away from the flame. This distribution of colors is representative of the distribution of DT_g/Dt. Gas velocity vectors are also shown [8].

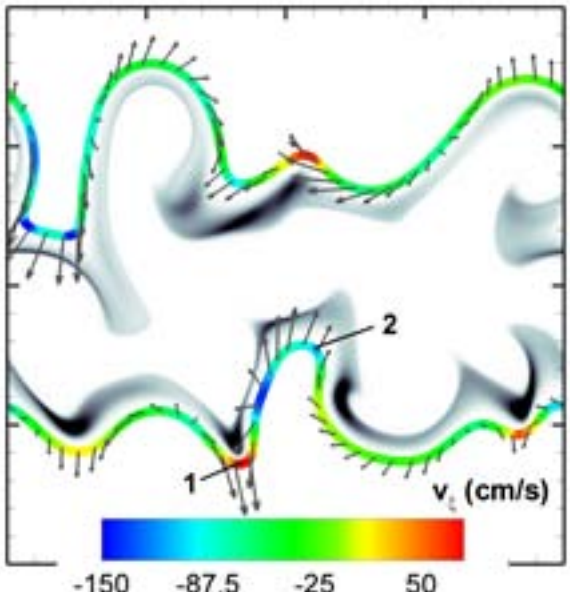

Figure 3. Soot contours (grayscale) with flame surface contour colored by relative velocity between the flame surface and the soot from 2-D DNS.

An analysis of this physics based on an alternate derivation of conditional-moment equations led to a relationship describing the aerosol mass fraction rate of change as a function of the conserved scalar [10-12] or equivalently for the present analysis as a function of the temperature. The key term resulting from this analysis was the contribution of flame diffusion relative to fixed fluid elements (aerosol particles with zero diffusivity) to the change in the aerosol environment that takes the form of

$$\frac{\partial}{\partial \eta}\left[\left\langle \nabla \cdot \left(\rho D \nabla \xi\right) Y_a \,|\, \eta \right\rangle P(\eta)\right] \tag{11}$$

where η is the conserved-scalar conditioning variable, $P(\eta)$ is the PDF of η, Y_a is the aerosol mass fraction and the brackets $\langle \cdot \,|\, \eta \rangle$ signify conditional averaging. This term describes the flux of particles to different conserved scalar values, or equivalently to different temperatures. The rate associated with this flux is the diffusive term $\nabla \cdot \left(\rho D \nabla \xi \right)$ so that in the current project we will also seek the statistics of this diffusive term through the analysis of joint distribution

$$P\left(\xi, \nabla \cdot \left(\rho D \nabla \xi \right) | \, \eta \left(T_g \right) \right) \tag{12}$$

that is the relevant joint distribution associated with the second term on the right-hand side of Eq. (4) (compare Eq. (10) for the first term in Eq. (4)). It is noteworthy that, because it involves two spatial derivatives, this term is dominated by the finest scales of turbulence so we expect the high-frequency component of this rate to be significant. That is, we expect to frequently see short times scales associated with the DT_g/Dt term in Eq. (4). The significance of this to the particle time-temperature histories is still to be determined.

ODT model comparisons with canonical flows

To obtain the statistics sought in the previous section, we will employ the ODT model in conjunction with a Lagrangian representation of the particle phase (described in the next section). The ODT model was first developed by Kerstein [1] as a one-dimensional representation of velocity and scalar fields that mimic key aspects of turbulent flows. In order to represent turbulent flows in a single dimension, a model for the nonlinear advection process leading to the turbulent cascade is required along with a rate for that nonlinear process. The model for the turbulent cascade is the triplet map, a conservative and nondissipative redistribution of the scalar and velocity fields that transfers fluctuations to smaller length scales, increases iso-scalar surface areas and increases shear rates. The rate of triplet maps is determined from the local shear energy (modified by viscous damping) that comes from the evolving velocity field. There have been several noteworthy advances in the basic formulation including a vector formulation that redistributes turbulent kinetic energy in a manner similar to pressure scrambling with an associated return to isotropy [2]. A variable density and spatially evolving formulation was subsequently introduced [3]. The model has been demonstrated in a number of non-reacting flows including homogeneous turbulence [1], mixing layers [2, 3, 13, 14], wakes [13], wall-boundary layers [15], and Rayleigh-Bernard convection [16].

The fact that the ODT model resolves the full range of reactive and diffusive scales has made it particularly useful in modeling turbulent combustion where it has been applied to a series of jet flames [17-20]. In conjunction with this work, we have extended the analysis of ODT model performance in turbulent combustion through comparisons with direct numerical simulations (DNS) [21]. Much of the focus in reacting flows with the ODT code has focused on fine-scale phenomena associated with diffusive mixing processes that are resolved in the ODT model and not in other approaches to CFD. The scalar-dissipation rate is a characteristic quantity associated with diffusive mixing processes.

A detailed study was conducted comparing ODT to DNS of mixing and reaction in three temporally-evolving planar ethylene jet flames with flame extinction and reignition processes. The three cases involved increasing levels of flame extinction (by changing the fuel/oxidizer composition), but were otherwise identical, with a jet Reynolds number of 5120. Ref. [21] provides a detailed description of

these flames and results. Validation of the ODT model was successful in this configuration, especially in regards to the jet evolution and diffusive mixing processes.

Figure 4 shows comparative results between the ODT and DNS for the stoichiometric mean and root mean square fluctuation of scalar dissipation rate—an important quantity in turbulence modeling and in Eqs. (8) and (9). The agreement of ODT with the DNS is very good, and lends confidence in the model to capture both fine scale mixing processes, and also the overall evolution of the flow, which was also achieved for this configuration.

As mentioned in the previous section, the ODT model has also been employed to model the evolution of soot in buoyant flames [9] and the results have been used to develop new models for flame aerosol transport [10, 11] that have also been validated using DNS [12].

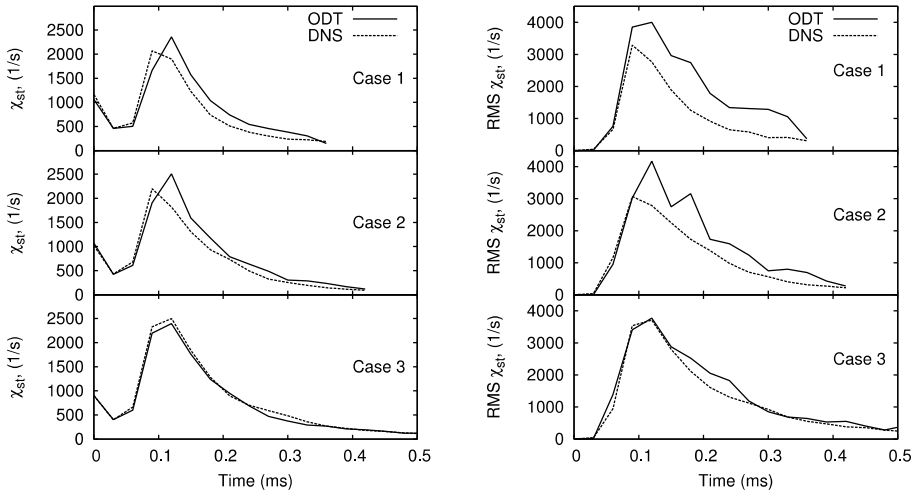

Figure 4. Mean (left) and root mean square (RMS, right) stoichiometric scalar dissipation rate as a function of time for three cases comparing ODT results to DNS.

Particle implementation in ODT code

Lagrangian particles were implemented in the ODT code as a major task of this first reporting period. The model is based on that of Schmidt et al. [22], who used ODT to study particle deposition in non-reacting flows. We have extended the model to include heat transfer properties, as well as capability for particle reactions. Here we give a description of the particle model implemented in the ODT code, and then present initial results of the model in homogeneous turbulent dispersion, and a planar mixing layer flame.

The ODT code consists of two concurrent processes: (1) evolution of unsteady diffusion-reaction equations for mass, momentum, energy, and scalar components (e.g. chemical species); (2) stochastic eddy events implemented using the triplet map described above that occur instantaneously and model turbulent advection. Details of the present ODT code and its implementation are available in Lignell et al. [23].

The particle evolution during diffusive advancement is similar to other Lagrangian particle approaches in which we integrate the particle drag law specifying particle velocity and position on the line. ODT, while one-dimensional, includes three velocity components (primarily used for specification of the eddy events). Likewise, while the particles are restricted to the ODT line, each particle has three components of velocity, and all three components are evolved, but only the in-line component contributes to the motion of the particle on the line. The particle position x and velocity u_p, are governed by

$$\begin{aligned} \frac{dx_p}{dt} &= u_p \\ \frac{du_p}{dt} &= -\frac{u_p - u_g}{\tau_p} f + g \end{aligned} \tag{12}$$

Here, x_p, and u_p are the particle position and velocity, respectively, g is gravity, and τ_p is the particle timescale given by

$$\tau_p = \frac{\rho_p d_p^2 C_c}{18\mu} \tag{12}$$

where ρ_p is the particle density, d_p is the particle diameter, μ is the fluid viscosity and C_c is the Cunningham slip factor. The factor f is a nonlinear correction factor for Reynolds number given by

$$f = \begin{cases} 1 & 0 < Re \le 1 \\ 1 + 0.15 Re^{0.687} & 1 < Re < 1000 \end{cases} \tag{12}$$

and C_c is given by

$$C_c = 1 + \frac{\lambda}{r_p}\left[1.127 + 0.4 e^{-1.1 r_p/\lambda}\right] \tag{12}$$

where λ is the fluid mean free path. The position and velocity equations are integrated with the other ODT line scalar equations using first or second order explicit methods. The gas velocity is assumed zero on the line (eddy events do the advecting and continuity for incompressible flow implies constant (zero) velocity). However, dilatation due to gas expansion from temperature and composition changes usually associated with combustion contributes to the gas velocity and must be computed. Particle temperatures are normally taken to be those of the surrounding fluid since particles are very small and response times are neglected. However, detailed particle heatup and reaction models are implemented including intraparticle temperature gradients computed by discrete solution of the unsteady 1-D heat equation with convective and radiative boundary conditions for each particle.

Particle transport during eddy events is somewhat more challenging. Eddy events in ODT occur instantaneously, but the transport effect on particles occurs due to drag over a period of time. To reconcile this, particle transport due to an eddy is implemented instantaneously, but the resultant particle velocity and location are computed by integrating the drag law over an eddy interaction time. Eddy events are characterized by a position x_e, a size L_e, and a timescale τ. Each location in an eddy is mapped to a new location according to the triplet map definitions in ODT. This local displacement is denoted Δx_e. An eddy velocity is created as $v_e = \beta\tau/\Delta x_e$, where $\beta\tau = \tau_{\square}$ is an eddy time. The parameter β is an adjustable

model constant. This is the gas velocity felt by the particles during the eddy event. Each particle in the eddy region will interact with the eddy for a time $\tau_i \leq \tau_e$. The interaction time will equal the eddy time if the particle remains in the eddy region for all of the eddy time. Otherwise, the interaction time is the time at which the particle trajectory takes it out of the eddy region. Equations (12) for particle velocity and position are integrated for the duration of the particle interaction time. This is done analytically and is very efficient. However, because the particle transport is implemented instantaneously but the drag law is integrated for the interaction time, the concurrent diffusive advancement would result in double integration of the particle drag law. To avoid this, the particle-eddy transport is computed due to the eddies alone by taking the difference of the integrated drag law solutions with and without the eddy velocity.

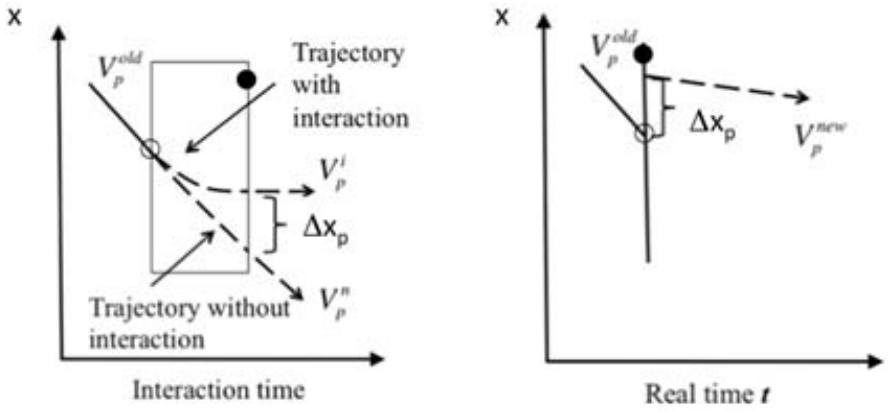

Figure 5. Particle trajectories during the eddy interaction time (left), and the real time coordinate in which eddy events are instantaneous (right). Open and closed circles show the initial and final fluid locations, respectively. The box indicates the eddy region in space-time.

Figure 5 illustrates the particle-eddy interaction process. The left and right plots sketch the particle trajectories in the eddy interaction (fictitious) and real time coordinates, respectively. The open and solid circles show the initial and final locations of fluid elements due to the triplet map. The rectangular box illustrates the eddy region. On the left plot of the figure, the particle trajectory is shown with and without the eddy displacement. The right plot shows the velocity and location of the particle before and after a triplet map. Note the instantaneous displacement of the particle due to the eddy displacement, and the slightly different instantaneous displacement of the fluid element.

A challenge arises when computing heat transfer between a gaseous fluid and a particle during a triplet map, that was not addressed in previous particle implementations in ODT. Again, this relates to the instantaneous eddy events inherent in the ODT model. While the heat transfer to the particle could be computed during the triplet map, it is less straight forward to compute the heat transfer from the gas due to the subsequent diffusion process. Indeed, one would have to mimic the full coupled diffusion/reaction process during the eddy event, which is not practical. An alternative approach is taken in which the relative velocity between the particle and gas during an eddy event is recorded for the given eddy, along with the end time of the eddy-particle interaction. During the diffusion processes, this relative velocity is used to compute the heat transfer coefficient using the Reynolds and Nusselt numbers, which enables

direct coupling between the gas and particle phases. Here, the Ranz-Marshall correlation is used: $Nu = 2+0.6Re^{1/2}Pr^{1/3}$, where Pr is the Prandtl number. Particles will often experience the velocity slip of several eddies simultaneously since eddy interaction regions in time and space will overlap. In this case, the cumulative effect is computed. Figure 6 shows particle trajectories and the eddy locations and time (left), along with the eddy particle interaction times (right) for which eddy velocities are used to compute heat transfer coefficients during the diffusion process. Note the eddy overlap region between eddies 1 and 2, during time interval marked Δt_2.

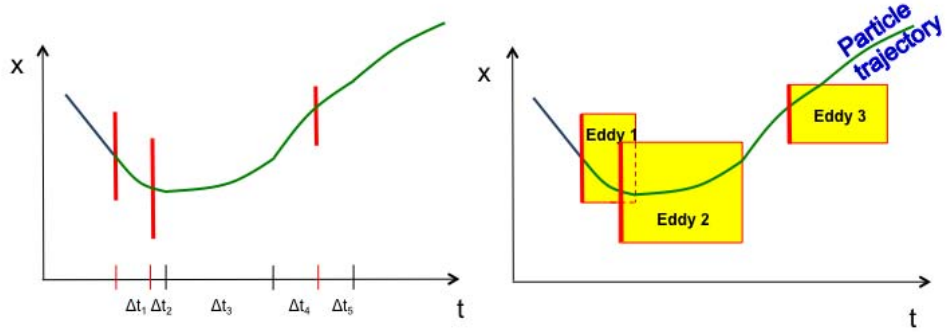

Figure 6. Illustration of eddy-overlap regions for computation of heat transfer coefficients. The left plot shows the particle path and the eddy locations. The right plot shows the eddy interaction regions.

Particle Simulation Results

Results of particle simulations are presented for two cases: (1) dispersion in homogeneous decaying turbulence; and (2) a reacting temporal mixing layer. The homogeneous turbulence results serve to validate the particle implementation model. This configuration is a classic canonical configuration for turbulence investigations. Simulation results are compared to the experiments of Snyder and Lumley [24]. The experiments consist of grid turbulence with a bar spacing of 2.54 cm and an average flow velocity of 6.55 m/s. Four particle types were used as shown in Table 1 with also gives the size and particle relaxation timescale. The simulations were performed by initializing a field of homogeneous turbulence by specifying a pseudo-random velocity field using Pope's model turbulent kinetic energy spectrum [25]. The spectrum was set to match the properties of the experiment with an integral scale of 2.54 cm, a velocity fluctuation of 4.7 m/s, and a Kolmogorov scale of 0.0391 mm. The energy spectrum and corresponding velocity profile are shown in Figure 7.

Table 1. Particle properties for homogeneous turbulence configuration.

Particle Type	Size (μm)	Relaxation timescale (ms)
Hollow Glass	46.5	1.58
Corn Pollen	87	21.2
Solid glass	87	53
Copper	46.5	53

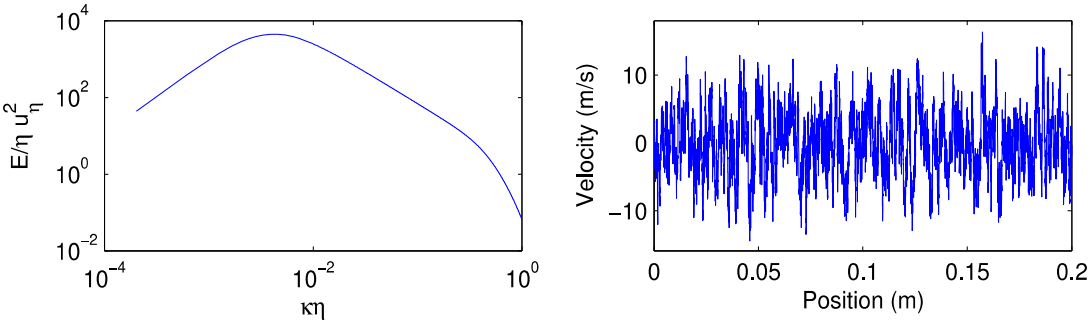

Figure 7. Energy spectrum and velocity field used in homogeneous turbulence simulations.

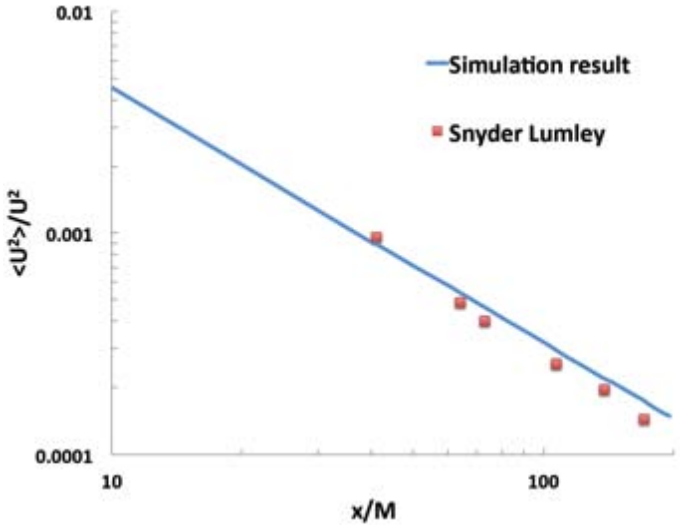

Figure 8. ODT and experimental decay of velocity fluctuations.

The evolution of the velocity decay is validated by comparing the root mean square (RMS) fluctuations of velocity between the experiments and simulation. These results are shown in Figure 8. The ODT eddy rate parameter C, is 2, the viscous penalty parameter Z is 100, and statistics were collected over 1024 ODT realizations. The agreement is very good. The ODT slope is slightly higher than the experimental, but this can be improved through adjustment of the ODT parameters.

Particle dispersion is computed by inserting single particles into the center of the domain and tracking the particle location as the flow evolves. For the particle simulations, the β parameter was set to 0.1, and 512 realizations were performed for each of the four particle types. Figure 9 shows results of the simulations and compares with the experimental measurements. The agreement is fairly good. For all particle types the dispersion increases with time (distance). Particles with smaller relaxation time scales have smaller Stokes number's and behave more like fluid particles, exhibiting higher dispersion. Particles with larger relaxation timescales (copper and solid glass) spread the least because of their higher Stokes numbers

(higher mass for a given size). The ODT captures both the trend and magnitude fairly well, but slightly over predicts the dispersion of the hollow glass and under predicts the dispersion of the copper particles and corn pollen. These results are comparable to other models of particle dispersion.

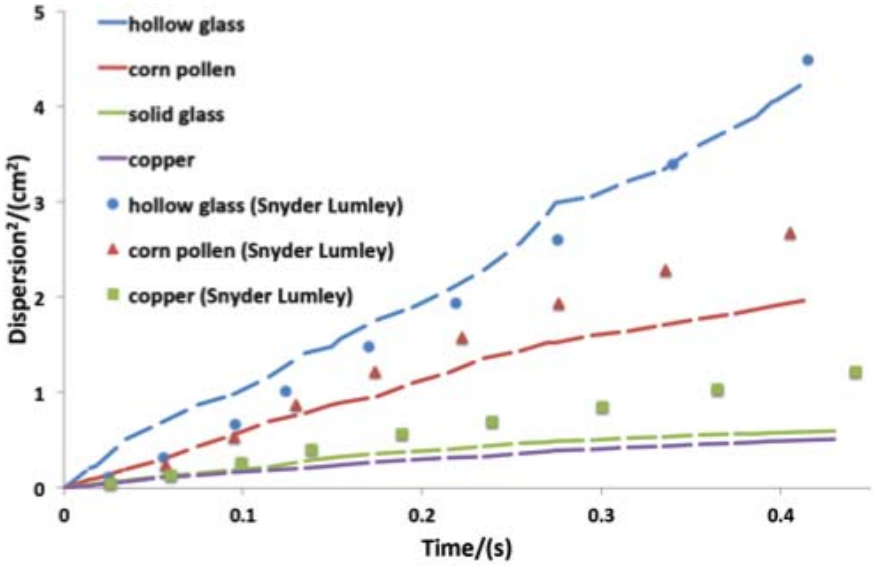

Figure 9. Comparison of ODT (lines) and experimental (symbols) particle dispersion in homogeneous turbulence. **Comparison of ODT (lines) and experimental (symbols) particle dispersion in homogeneous turbulence.**

The second illustrative case presented is a turbulent mixing layer flame in which the oxidizer flows on the left and the fuel on the right of a splitter plane. The mixing layer is another canonical flow that allows gathering of particle temperature statistics in a simple configuration for validation. As with the homogeneous case (which can easily accommodate reactions as well), mixing statistics such as large and fine mixing timescales and particle locations can be easily varied. The velocity difference between the streams is 196 m/s. The stream temperatures are at 550 K, with ethylene as the fuel and air as the oxidizer. 1000 particles are randomly distributed on the 1.5 cm domain. The particle relaxation timescales are 0.5 ms, resulting in a St≈10. These results provide a first look at particle statistics in the reacting flow. Of particular interest will be the motion of the particles relative to particular iso-contours of the temperature, along with the joint particle temperature time PDF as discussed above.

Figure 10 shows the mean temperature contours of a portion of the mixing layer domain. Overlaid on these contours are particle paths for a single realization of the flow. Only half of the particles are shown for clarity. Note that the motion of the particles during eddy events appears as rapid horizontal motions. The statistics of these motions are the desired output and are representative of turbulent motions. The particles move through the flow crossing individual flame elements, which exchange heat between the gas and particle phases. Note the relatively fewer eddy events in the high temperature regions where viscosity and dilatation are highest. The degree of spread of the particles depends upon the Stokes number, with ligher particles spreading more than heavy particles, consistent with results from the homogeneous turbulence dispersion discussed above. The particles on the edges appear to spread from the centerline with time. This is due to the dilatation of the flow as combustion causes decreased density with heat release. The spreading of the mixing layer is also evident in the temperature “fan” and a decrease in the peak mean temperatures due to the fluctuations is observed. The temperatures of

individual instantaneous flamelets are relatively constant here, affected primarily through dissipative mixing, usually modeled using the scalar dissipation rate discussed above, but captured directly in ODT.

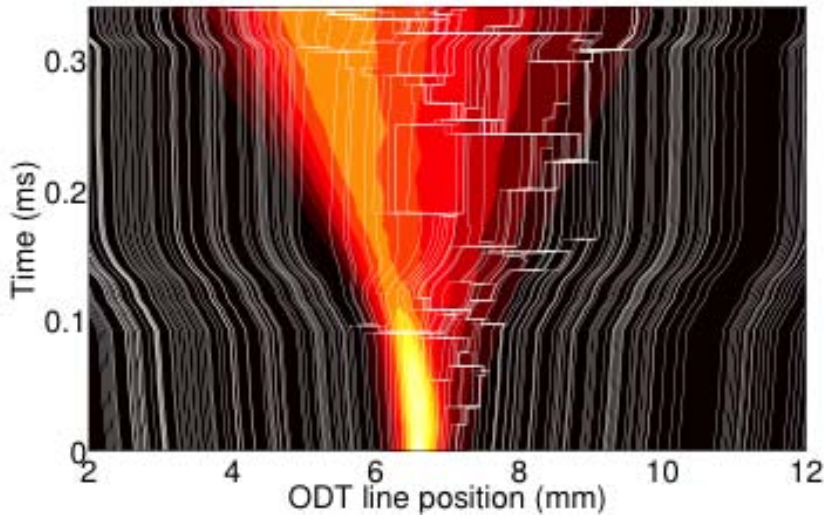

Figure 10. Mixing layer mean temperature contours with instantaneous particle paths overlaid.

Looking forward

The present reporting period was primarily devoted to the particle model implementation and validation. Moving forward detailed statistical investigations will be performed to analyze the quantities described in the Statistics of particle time-temperature histories section. As an example of statistical quantities that may be computed, the mixing layer simulations were processed to compute the fraction of particles in the domain that spend a cumulative time greater than 0.03 ms above a given temperature. This temperature might be regarded as a critical temperature and the particle fraction noted denoted a "kill fraction" if the particle heating time constant, τ_h, is of this order. Figure 11 shows this "kill fraction" for the mixing layer simulation. The fraction is unity at 550 K as this is temperature of the fuel and oxidizer stream. For higher temperatures, fewer and fewer of the particles experience durations above the given temperature greater than 0.03 ms.

More complete descriptions can be reported at a given temperature. For example, at 1000 K a full time PDF may be computed for the particles. Results can be conditioned on initial particle location relative to the flame. Figure 12 shows, for the mixing layer case, a histogram of percent of particles spending given times above four critical temperatures. The shapes and magnitudes of these PDFs will provide insights into particle deactivation in turbulent mixing environments. The determination of statistical requirements has been presented in previous sections, is expected to be ongoing through the project and will evolve as analysis of results suggest future directions.

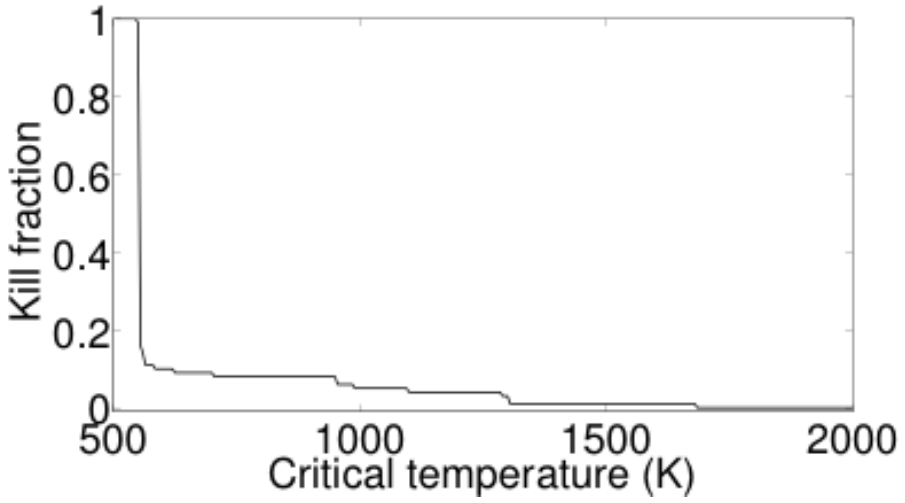

Figure 11. Fraction of particles spending a cumulative time greater than 0.03 ms above a given critical temperature.

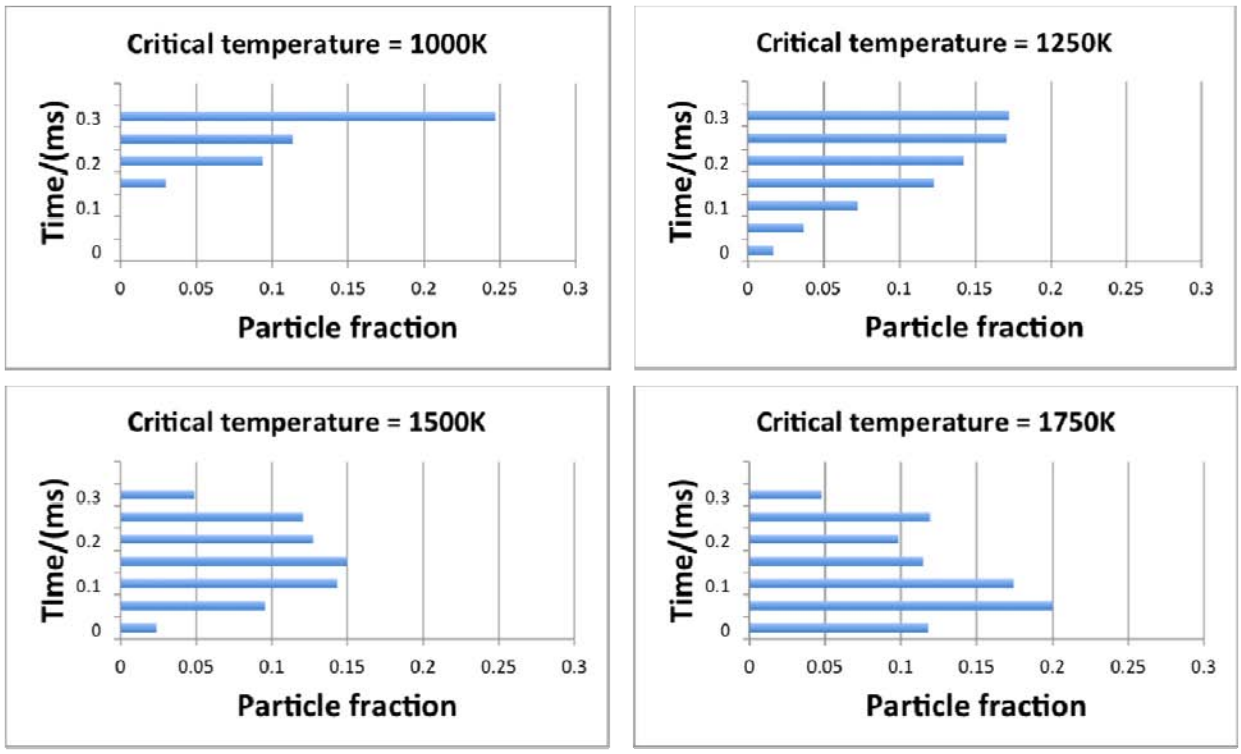

Figure 12. Fraction of particles spending the indicated time above four temperatures as indicated.

Project statistics

In this reporting period support has been provided to the principal investigator at Sandia National Laboratories and to the co-principal investigator, a graduate student and an undergraduate student at Brigham Young University. We have published one paper in conjunction with this work .

Summary

This report describes the first stages taken to predict the statistics of particle time-temperature histories relevant to neutralization of particles through exposure to high temperature environments. In addition to the statistics of the temperature distribution, the statistics of the time that particles are exposed to high-temperature gases are of interest, leading to a primary focus on the joint statistics of temperature and time scale $P(T_g, \Delta t)$. To predict the statistics of exposure time scale, the gradients and diffusive-reactive time scales have been identified as of interest, at least when particle heating times are not fast relative to flow time scales. Since temperature has a strong source term in many flows, and since this source term is difficult to resolve in traditional approaches to CFD, we have related the temperature gradient and time scale statistics to the statistics of conserved scalars that are easier to obtain in the context of CFD. The joint distributions of interest for large particles (Stokes numbers much greater than unity) are the joint distributions of a scalar and its gradient, $P\left(\xi, \nabla\xi\right)$. For small particles (Stokes numbers much less than unity) the statistics of interest are the joint distributions of a scalar and its diffusive rate of change, $P\left(\xi, \nabla\cdot\left(\rho D\nabla\xi\right)\right)$. The results presented in terms of temperature are expected to be extensible to other thermochemical insults.

To collect the statistical quantities of interest, we will employ the ODT model. Prior results with the ODT model have been reviewed, and we have addressed prediction of gradients, relevant to the interaction time scales, through comparison with DNS results. Lagrangian particle tracking has been implemented within the context of ODT to allow collection of statistics for particles that move relative to fluid elements (finite slip velocities), and this implementation has been evaluated through predictions of classical particle dispersion results. In addition to the particle dispersion aspects of the ODT-Lagrangian-particle implementation, we have developed a new approach to predicting heat transfer to particles in the ODT simulation environment. We have also carried out sample simulations of particle histories in a reacting shear layer where particles are exposed to a spreading flame brush to begin our investigation of the particle parameter space.

References

[1] A. R. Kerstein, "One-dimensional turbulence: Model formulation and application to homogenous turbulence, shear flows, and buoyant stratified flows," *J. Fluid Mech.*, vol. 392, pp. 277-334, 1999.

[2] A. R. Kerstein, W. T. Ashurst, S. Wunsch, and V. Nilsen, "One-dimensional turbulence: vector formulation and application to free shear flows," *J. Fluid Mech.*, vol. 447, pp. 85-109, 2001.

[3] W. T. Ashurst and A. R. Kerstein, "One-dimensional turbulence: Variable-density formulation and application to mixing layers," *Phys. Fluids*, vol. 17, p. 025107, 2005.

[4] A. Y. Klimenko and R. W. Bilger, "Conditional Moment Closure for Turbulent Combustion," *Prog. Energy Combust. Sci.*, vol. 25, pp. 595-687, 1999.

[5] N. Peters, *Turbulent Combustion*: Cambridge University Press, 2000.

[6] L. Vervisch and D. Veynante, "Interlinks Between Approaches for Modeling Turbulent Flames," *Proc. Combust. Inst.*, vol. 28, pp. 175-183, 2000.

[7] E. Van Kalmouth and D. Veynante, "Direct numerical simulations analysis of flame surface density models for nonpremixed combustion," *Physics of Fluids*, vol. 10, p. 2347, 1998.

[8] D. O. Lignell, J. H. Chen, P. J. Smith, T. Lu, and C. K. Law, "The effect of flame structure on soot formation and transport in turbulent nonpremixed flames using direct numerical simulation," *Comb. Flame*, vol. 151, pp. 2-28, 2007.

[9] A. J. Ricks, J. C. Hewson, A. R. Kerstein, J. P. Gore, S. R. Tieszen, and W. T. Ashurst, "A spatially developing one-dimensional turbulence (ODT) study of soot and enthalpy evolution in meter-scale buoyant turbulent flames," *Combustion Science and Technology,* vol. 182, pp. 60-101, 2010.

[10] J. C. Hewson, A. J. Ricks, S. R. Tieszen, A. R. Kerstein, and R. O. Fox, "Conditional-Moment Closure with Differential Diffusion for Soot Evolution in Fires.," in *Studying Turbulence Using Numerical Simulation Databases - XI, Proceeding of the 2006 Summer Program*, ed Stanford, CA: Center for Turbulence Research, 2006, pp. 311-324.

[11] J. C. Hewson, A. J. Ricks, S. R. Tieszen, A. R. Kerstein, and R. O. Fox, "On the Transport of Soot Relative to a Flame: Modeling Differential Diffusion for Soot Evolution in Fire.," in *Combustion Generated Fine Carbonaceous Particles*, H. Bockhorn, A. D'Anna, A. F. Sarofim, and H. Wang, Eds., ed Karlsruhe, Germany: Karlsruhe University Press, 2009, pp. 571-587.

[12] D. O. Lignell, J. C. Hewson, and J. H. Chen, "A-Priori Analysis of Conditional Moment Closure Modeling of a Temporal Ethylene Jet Flame with Soot Formation Using Direct Numerical Simulation," *Proc. Combust. Instit.,* vol. 32, pp. 1491-1498, 2009.

[13] A. R. Kerstein and T. D. Dreeben, "Prediction of turbulent free shear flow statistics using a simple stochastic model," *Phys. Fluids,* vol. 12, pp. 418-424, 2000.

[14] W. T. Ashurst, A. R. Kerstein, L. M. Pickett, and J. B. Ghandhi, "Passive scalar mixing in a spatially developing shear layer: Comparison of one-dimensional turbulence simulations with experimental results," *Physics of Fluids,* vol. 15, pp. 579-582, Feb 2003.

[15] T. D. Dreeben and A. R. Kerstein, "Simulation of vertical slot convection using 'one-dimensional turbulence'," *International Journal of Heat and Mass Transfer,* vol. 43, pp. 3823-3834, Oct 2000.

[16] S. Wunsch and A. R. Kerstein, "A stochastic model for high-Rayleigh-number convection," *Journal of Fluid Mechanics,* vol. 528, pp. 173-205, Apr 10 2005.

[17] T. Echekki, A. R. Kerstein, T. D. Dreeben, and J. Y. Chen, "'One-dimensional turbulence' simulation of turbulent jet diffusion flames: Model formulation and illustrative applications," *Combustion and Flame,* vol. 125, pp. 1083-1105, May 2001.

[18] J. C. Hewson and A. R. Kerstein, "Stochastic Simulation of Transport and Chemical Kinetics in Turbulent CO/H2/N2 Flames," *Combust. Theory Modeling,* vol. 5, pp. 669-697, 2001.

[19] J. C. Hewson and A. R. Kerstein, "Local Extinction and Reignition in Nonpremixed Turbulent $CO/H_2/N_2$ Jet Flames," *Combust. Sci. Tech.,* vol. 174, pp. 35-66, 2002.

[20] J. C. Hewson, A. R. Kerstein, and T. Echekki. (2002). *One-Dimensional Stochastic Simulation of Advection-Diffusion-Reaction Coupling in Turbulent Combustion*.

[21] D. O. Lignell and D. S. Rappleye, "One-dimensional turbulence simulation of flame extinction and reignition in planar ethylene-jet flames," *Comb. Flame,* 2012.

[22] J. R. Schmidt, J. O. L. Wendt, and A. R. Kerstein, "Prediction of particle laden turbulent channel flow using one dimensional turbulence," in *Proceedins of the IUTAM Symposium on Computational Approaches to Disperse Multiphase Flow, Argonne, IL,* 2004.

[23] D. O. Lignell, A. R. Kerstein, G. Sun, and E. I. Monson, "Mesh adaption for efficient multiscale implementation of One-Dimensional Turbulence," *Theoretical and Computational Fluid Dynamics,* 2012.

[24] W. H. Snyder and J. L. Lumley, "Some measurements of particle velocity autocorrelation functions in a turbulent flow," *Journal of Fluid Mechanics,* vol. 48, pp. 41-71, 1971.

[25] S. B. Pope, *Turbulent Flows*. Cambridge: Cambridge University Press, 2000.

Distribution (electronic)

1 Defense Threat Reduction Agency
Attn: Dr. S. Peiris
RD-BAS, Cube 3645E
8725 Kingman Road
Fort Belvoir, VA 22060-6201
Suhithi.Peiris@dtra.mil

1 Brigham Young University
Attn: Prof. David Lignell
350 Clyde Building
Provo, UT 84602
davidlignell@byu.edu

1	MS0836	John Hewson	1532
1	MS1135	Randy Watkins	1532
1	MS1135	Allen Ricks	1532
1	MS1135	Josh Santarpia	1532
1	MS0899	Technical Library	9536


Sandia National Laboratories